

Spectroscopy of the parametric magnons excited by 4-wave process

G. de Loubens, V. V. Naletov, V. Charbois, and O. Klein

*Service de Physique de l'État Condensé,
CEA Orme des Merisiers, F-91191 Gif-Sur-Yvette*

V. S. Tiberkevich and A. N. Slavin

Department of Physics, Oakland University, Michigan US-48309

(Dated: October 28, 2018)

Abstract

Using a Magnetic Resonance Force Microscope, we have performed ferromagnetic resonance (FMR) spectroscopy on parametric magnons created by 4-wave process. This is achieved by measuring the differential response to a small source modulation superimposed to a constant excitation power that drives the dynamics in the saturation regime of the transverse component. By sweeping the applied field, we observe abrupt readjustment of the total number of magnons each time the excitation coincides with a parametric mode. This gives rise to ultra-narrow peaks whose linewidth is lower than $5 \cdot 10^{-6}$ of the applied field.

The detailed understanding of the non-linear (NL) regime of the magnetization dynamics is important both from a fundamental point of view¹ but also for applications in spintronic devices². Interest resides in the exact nature of the parametric modes that are excited above the supercriticality threshold. Recent experiments performed on a yttrium iron garnet (YIG) film have shown that these parametric magnons can form a Bose-Einstein condensate³ under high power pumping. It was also demonstrated that their energy decay rate to the lattice is substantially diminished compared to the long wavelength modes⁴, which are usually studied by FMR. In this paper, it will be shown that it is also possible to measure the FMR spectrum of these parametric magnons despite the fact that these high k -vector spin-waves do not overlap with the homogeneous microwave field. This is achieved by saturating the dynamics of the mode that couples to the microwave. Any additional power that is injected in the spin system flows directly towards the excitation of these parametric magnons. Since each parametric mode has a different feedback influence on the saturation, it is possible, by sweeping an external parameter, to detect the point where the transfer from one parametric mode to another takes place. But the induced effects are small and detecting them requires both a sensitive and precise measurement setup.

Our detection of the dynamical response uses a mechanical-FMR setup working at room temperature^{5,6}. This scheme is inspired by local probe techniques. The static component of the disk magnetization, $M_z = M_s \cos \theta$, is coupled through the dipolar interaction to a magnetic probe attached at the end of a soft cantilever, whose deflection is monitored. Exciting the sample at a fixed frequency, spectroscopy is achieved by recording the cantilever motion as a function of the perpendicular dc applied field, H_{ext} , which is produced by a NMR electromagnet. The variation of force on the cantilever is proportional to the total number of magnons excited at resonance, N_t , with $N_t \equiv (M_s - M_z)/(\gamma \hbar)$. Further details about the mechanical-FMR experiment can be found in Ref.⁷.

Driving the dynamics of ferromagnets in the NL regime requires to cant the magnetization, M_s , away from its equilibrium axis by an angle θ exceeding a couple of degrees. Only powerful HF source can produce such large excitation amplitude⁸. Improvement of the efficiency can be gained with microstrip cavities, where the HF energy is concentrated in smaller volume. A schematic of our setup is shown in Fig.1(a). It comprises a 0.5mm wide Au stripline fabricated by U.V. lithography and deposited on a 0.5mm thick alumina substrate whose bottom layer is a conducting ground plane. An impedance matched cavity

(half-wavelength) is created by etching a $32\mu\text{m}$ gap across the stripe. The HF source is tuned at the cavity frequency ($\omega_s/2\pi = 10.47\text{GHz}$) set by the length (5mm) of the isolated segment. The sample is a $t = 4.75\mu\text{m}$ thick YIG single crystal. The YIG film is ion milled into a disk of diameter $\phi = 160\mu\text{m}$ and placed at the center of the cavity. The homogeneous external static field H_{ext} , well above the saturation field, is applied parallel to the disk axis.

This work concentrates on the 4-magnons coupling term in the equation of motion of the magnetization. It becomes the dominant term once the premature saturation regime of the microwave susceptibility is achieved⁹. From previous experiments on the same sample⁴, we have established that the saturation threshold occurs at excitation power above -35dBm for our setup. Fig.1(b) shows the static deflection of the cantilever as a function of H_{ext} when $P_{\text{max}} = -10.8$ dBm. The trace corresponds to the lineshape of the uniform mode¹⁰ in the foldover regime. Hysteretic behaviors are a standard signature of NL effects, where the eigen-frequency of the resonance depends on the amplitude of the excitation¹¹. Foldover effects in magnetic materials have been explained by Anderson and Suhl in 1955¹². The features of interest are the tiny steps observed in the wings of the resonance (see insert of Fig.1(b)). These jumps are not random. They are reproducible and occur regularly in field.

A more detailed picture can be obtained by measuring the differential response. We detect here the response to a source modulated excitation around the saturation regime. The power level follows the time dependence $P(t) = P_{\text{max}} \left\{ 1 + \frac{\epsilon}{2}(\sin(\omega_c t) - 1) \right\}$, where the modulation frequency is set at the resonance frequency of the cantilever. This frequency is much lower than all the damping rates of the spin system. In this case, the differential part of the mechanical signal is amplified by $Q = 4500$, the quality factor of the mechanical resonator. Fig.1(c) is the pattern recorded by a lock-in when the modulation amplitude is 0.5% ($\epsilon = 5 \cdot 10^{-3}$) of the maximum power, $P_{\text{max}} = -17$ dBm. It corresponds to a source modulation of less than 50nW in amplitude. The spectrum shown here is a zoom on a 2G sweep of H_{ext} in the reversible region of the static signal. We observe about ten ultra-narrow lines (width 30mG) regularly spaced every 60mG. Such sharp peaks resemble the parametric excitations observed by Jantz and Schneider in 1975 in the subsidiary absorption of YIG films¹³ (3-wave process). To the best of our knowledge, this is, however, the first time that they are observed at resonance.

The striking characteristics of these peaks is their narrowness. This 30mG broadening is much smaller than the FMR linewidth $\Delta H = 1.2\text{G}$ measured in the linear regime on

the same sample¹⁴. Further insight can be obtained by looking at the shape of the signal (see Fig.2a) for different modulation depth, ϵ , at constant maximum power P_{\max} . Fig.2b shows that the broadening B of the parametric peaks is clearly proportional to ϵ . Foldover effects establish a coupling between the HF power and the resonance frequency. Thus source modulation in the NL regime produces also a frequency modulation. But in FMR, there is no difference between frequency modulation and a modulation of the applied field, since both are coupled by the gyromagnetic ratio. Fig.1c can thus be seen as the differential characteristics of Fig.1b, where the depth of modulation is proportional to ϵ . At very low ϵ eventually the intrinsic broadening should be seen. Although a NMR electromagnet with a 10^{-6} precision in H_{ext} has been used, the fact that B extrapolates linearly down to the smallest value of ϵ reached by our setup, suggests that the intrinsic part of the broadening has not been measured here.

For completeness, we show in Fig.3 how the instability region evolves when the dc bias P_{\max} is increased at constant ϵ . We observe an increase of the applied field window, where parametric peaks occur. The size of the window follows monotonically the amplitude of the dc power *i.e* how far we depart from the supercriticality threshold.

In the following, we propose an analytical framework to account for the main features observed experimentally. Saturation phenomena can be caused by a multitude of nonlinear processes: nonlinear dissipation, nonlinear phase mechanism, nonlinear energy feedback effect. In many cases several of these mechanisms, as well as nonlinear frequency shift, need to be accounted simultaneously for the correct description of the phenomenon. The most probable limiting mechanism in the case of perpendicular pumping is the nonlinear energy feedback. This mechanism is described by a 4-magnons interaction ($\xi_k b_0^2 b_k^* b_{-k}^* + \text{c.c}$) in the Hamiltonian of the system. It represents second-order parametric excitation of the pair of plane spin waves (b_k, b_{-k}) by the uniform precession (b_0). Suhl showed in 1957, the equations of motion for the amplitudes b_k of the plane spin waves have the form:

$$\dot{b}_k = -i\omega_k b_k - i\xi_k b_0^2 b_{-k}^* - \eta_k b_k, \quad (1)$$

where η_k is its *energy* decay to the lattice (the index must allow for k -dependent relaxation rates^{4,15}). The equation for the amplitude b_0 of the uniform precession is given by

$$\dot{b}_0 = -i\omega_0 b_0 - i \sum_k \xi_k b_k b_{-k} b_0^* - \eta_0 b_0 + \gamma h e^{-i\omega_s t}. \quad (2)$$

where the last term is the excitation field $h = \sqrt{P}$. The term $\sum_k \dots$ describes nonlinear feedback effect of all the parametric waves on the uniform precession. This term gives effective nonlinear dissipation for b_0 . In the following, we will be looking at harmonics solution where all the spin-waves precess synchronously: $\dot{b}_k = -i\omega_s b_k$.

As one can see from Eq. (1), an instability (exponential growth of the population) occurs if the effective damping of at least one parametric mode becomes negative:

$$|b_0|^4 > \frac{(\omega_k - \omega_s)^2 + \eta_k^2}{\xi_k^2}. \quad (3)$$

Growth of b_k will create effective damping for the uniform mode b_0 (through the $\sum_k \dots$ term in Eq. (2)), which will reduce b_0 to its threshold value:

$$|b_0|^2 = N_0 \equiv \min_k \frac{\sqrt{(\omega_k - \omega_s)^2 + \eta_k^2}}{\xi_k}, \quad (4)$$

Determination of the mode that will grow unstable depends on the coupling ξ_k , which is maximum $\xi_k/\gamma = 2\pi M_s (\approx 900\text{G})$ for k propagating parallel to the magnetization direction⁹. As shown on the magnon manifold drawn in Fig.4, these longitudinal SW have a wavevector $k_{\max} = \sqrt{N_{\perp} 4\pi M_s^2 / (2A)} \approx 6.3 \cdot 10^4 \text{cm}^{-1}$, where A is the exchange constant and N_{\perp} is the transverse depolarization factor. For our disk, it corresponds to a standing spin-wave confined across the thickness with about 5 nodes along it. In this model, the threshold power is given by the analytical formula, $h_c^2 = \eta_k \Delta H^2 / \xi_k$ and the calculated value $h_c = 5 \text{mOe}$ agrees with the the onset of saturation measured experimentally⁴.

Sweeping the bias magnetic field H_{ext} (or ω_s) changes the nature of the parametric mode that grows unstable, as the minimum in Eq. (4) occurs for different value of k . Finite size-effects introduce a discretisation in k -space of all the SW. The frequency separation $\Delta\omega$ between two nearby normal mode is about $\Delta\omega = 4\gamma A k \Delta k / M_s$, where $\Delta k = \pi/\phi$ corresponds to the quantification of the k -vector along the largest sample dimension. The parametric modes have thus a principal wvector $k_{\max} \parallel M_s$, with a small additional component Δk in the disk plane. We find numerically $\Delta\omega/\gamma = 0.12\text{Oe}$, a predicted separation twice as large as what is observed experimentally in Fig.1(c). The value of k_{\max} however depends strongly on the angle of propagation of the degenerate magnons. A deviation of about 7° of their propagation direction compare to the normal of the disk will be enough to explain the discrepancy.

The amplitude of the steps can also be estimated analytically with an approximated model. Assuming that only one pair of parametrically coupled waves dominates all the

others, then its amplitude can be inferred from Eq. (2). If the mode b_k is excited, then its amplitude will grow to the level:

$$|b_k|^2 = |b_{-k}|^2 = N_k \equiv \frac{\sqrt{(\gamma h)^2 \xi_k^2 N_0 - \{(\omega_k - \omega_s)\eta_0 + (\omega_0 - \omega_s)\eta_k\}^2 + (\omega_0 - \omega_s)(\omega_k - \omega_s) - \eta_0 \eta_k}}{N_0 \xi_k^2}, \quad (5)$$

that provide the effective damping to fix N_0 at the level given by Eq. (4). The number of magnons in the majority mode N_k changes *abruptly* with the change of the excited mode due to the sweep of the magnetic field. In the differential graphs this will lead to a singularity at the points, where the transfer from one excited mode to another takes place. In reality, due to the presence of the thermal noise and other nonlinear processes (that are ignored here) one will observe a sharp (intrinsically broaden) peak at the points where the transfer from one excited mode to another occurs.

To see this more clearly, let us assume that coupling coefficients of all modes are the same, $\xi_k = \xi$. Then the changes of the parametrically excited modes (say, modes 1 and 2) will be at such a magnetic field, that $(\omega_1 - \omega_s) = -(\omega_2 - \omega_s) = \Delta\omega/2$ (see Eq. (4)).

Assuming that $|\omega_0 - \omega_s| \ll \eta_k$ and $\Delta\omega \ll \eta_k$ we can write $N_0 \approx \eta_k/\xi$ and, approximately,

$$N_{1,2} \approx (\zeta - 1) \frac{\eta_0}{\xi} \pm \frac{(\zeta - 1)}{\zeta} \frac{(\omega_0 - \omega_s) \Delta\omega}{2\xi\eta_k}, \quad (6)$$

where $\zeta \equiv h/h_{cr}$ is the supercriticality parameter of the microwave magnetic field.

Thus, the total number of spin wave modes differ by

$$\Delta N_t \equiv N_1 - N_2 = \frac{(\zeta - 1)}{\zeta} \frac{(\omega_0 - \omega_s) \Delta\omega}{\xi\eta_k}, \quad (7)$$

which will give small "steps" (of the order of 1% of N_t) in the behavior of $M_z(H_{ext})$ at different "integral" characteristics and ultranarrow peaks at "differential" characteristics of M_z vs. H_{ext} . These analytical findings are in good agreement with the experimental observed in Fig.1.

In conclusion, we have achieved FMR spectroscopy of parametric magnons. The observed linewidth of 30 mG corresponds to a lifetime of the order of $2\mu s$, which should be compared with the spin-lattice relaxation rate $T_1 = 106 ns$ usually observed in the linear regime¹⁴. Such long lifetime starts to become comparable to the one found in nuclear magnetic resonance using shimmed magnets. This result opens up the possibility of making

ultra-stables Yig Tuned Oscillators or ultra-sensitive absolute magnetic field detectors using these parametric resonances.

-
- ¹ A. N. Slavin and V. S. Tiberkevich, Phys. Rev. B **74**, 104401 (pages 4) (2006), URL <http://link.aps.org/abstract/PRB/v74/e104401>.
 - ² G. A. Prinz, J. Magn. Magn. Mater. **200**, 57 (1999).
 - ³ S. O. Demokritov, V. E. Demidov, O. Dzyapko, G. A. Melkov, A. A. Serga, B. Hillebrands, and A. N. Slavin, Nature **443**, 430 (2006), URL <http://www.nature.com/doifinder/10.1038/nature05117>.
 - ⁴ G. de Loubens, V. V. Naletov, and O. Klein, Physical Review B (Condensed Matter and Materials Physics) **71**, 180411 (pages 4) (2005), URL <http://link.aps.org/abstract/PRB/v71/e180411>.
 - ⁵ Z. Zhang, P. C. Hammel, and P. E. Wigen, Appl. Phys. Lett. **68**, 2005 (1996).
 - ⁶ V. Charbois, V. V. Naletov, J. Ben Youssef, and O. Klein, Appl. Phys. Lett. **80**, 4795 (2002).
 - ⁷ V. V. Naletov, V. Charbois, O. Klein, and C. Fermon, Appl. Phys. Lett. **83**, 3132 (2003).
 - ⁸ S. Y. An, P. Krivosik, M. A. Kraemer, H. M. Olson, A. V. Nazarov, and C. E. Patton, J. Appl. Phys. **96**, 1572 (2004).
 - ⁹ H. Suhl, J. Phys. Chem. Solids **1**, 209 (1957).
 - ¹⁰ V. Charbois, V. V. Naletov, J. Ben Youssef, and O. Klein, J. Appl. Phys. **91**, 7337 (2002).
 - ¹¹ V. S. L'vov, *Wave turbulence under parametric excitation* (Springer, Berlin, 1994).
 - ¹² P. W. Anderson and H. Suhl, Phys. Rev. **100**, 1788 (1955).
 - ¹³ W. Jantz and J. Schneider, Phys. Stat. Sol. (a) **31**, 595 (1975).
 - ¹⁴ O. Klein, V. Charbois, V. V. Naletov, and C. Fermon, Phys. Rev. B (Rapid Comm.) **67**, 220407 (2003).
 - ¹⁵ U. Hoeppe and H. Benner, Physical Review B (Condensed Matter and Materials Physics) **71**, 144403 (pages 7) (2005), URL <http://link.aps.org/abstract/PRB/v71/e144403>.

Figures

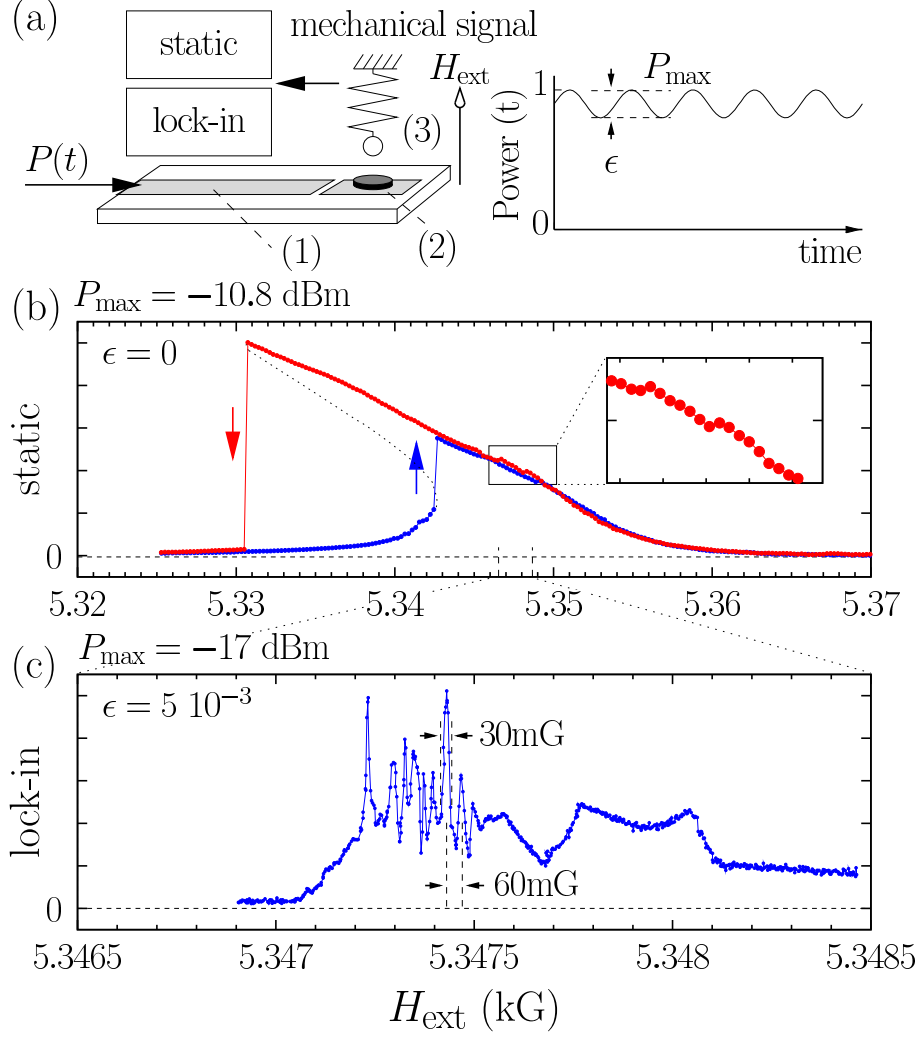


FIG. 1: (a) Schematic of the microstrip circuit (1). The FMR spectrum of a micron-size YIG disk (2) is detected by Magnetic Resonance Force Microscopy (3). On the right is shown $P(t)$, the waveform of the power injected in the microwave circuit (1). The amplitude of the sinusoidal modulation is $\epsilon P_{\max}/2$. (b) Static deflection of the cantilever as a function of H_{ext} . The trace is the lineshape of the uniform mode in the foldover regime. (c) Vibration amplitude of the cantilever measured by a lock-in synchronous with source modulation. The differential characteristics reveals the parametric excitation spectrum.

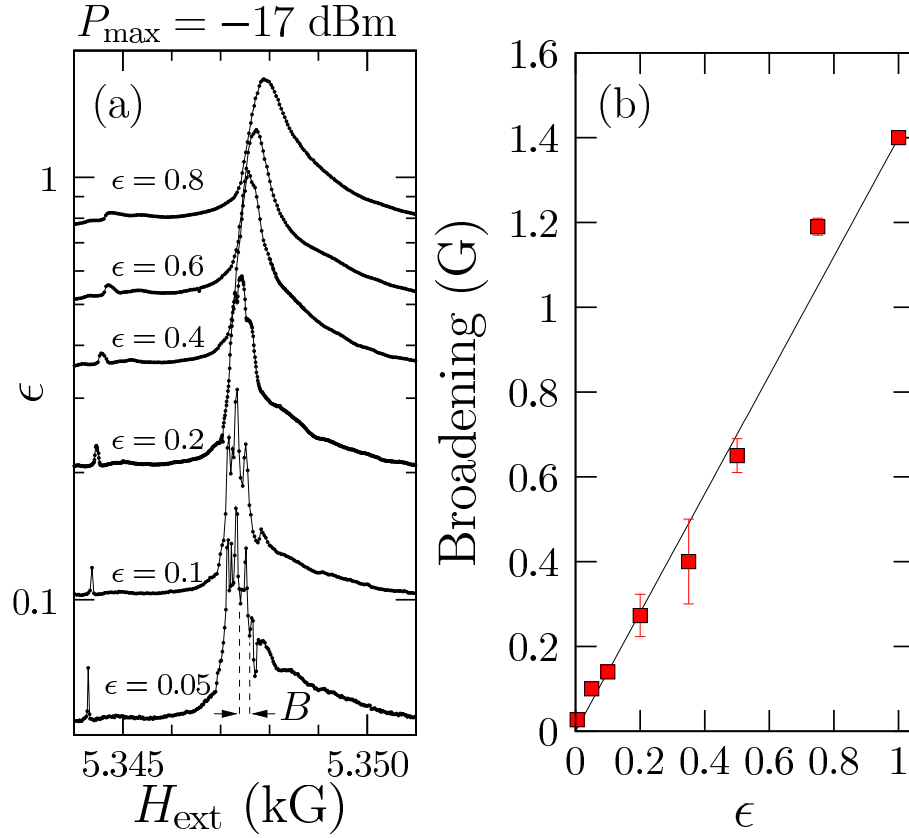


FIG. 2: (a) Differential spectrum as a function of the modulation depth ϵ (constant $P_{\text{max}} = -17$ dBm). B is the broadening of the parametric peaks. (b) B as a function of ϵ .

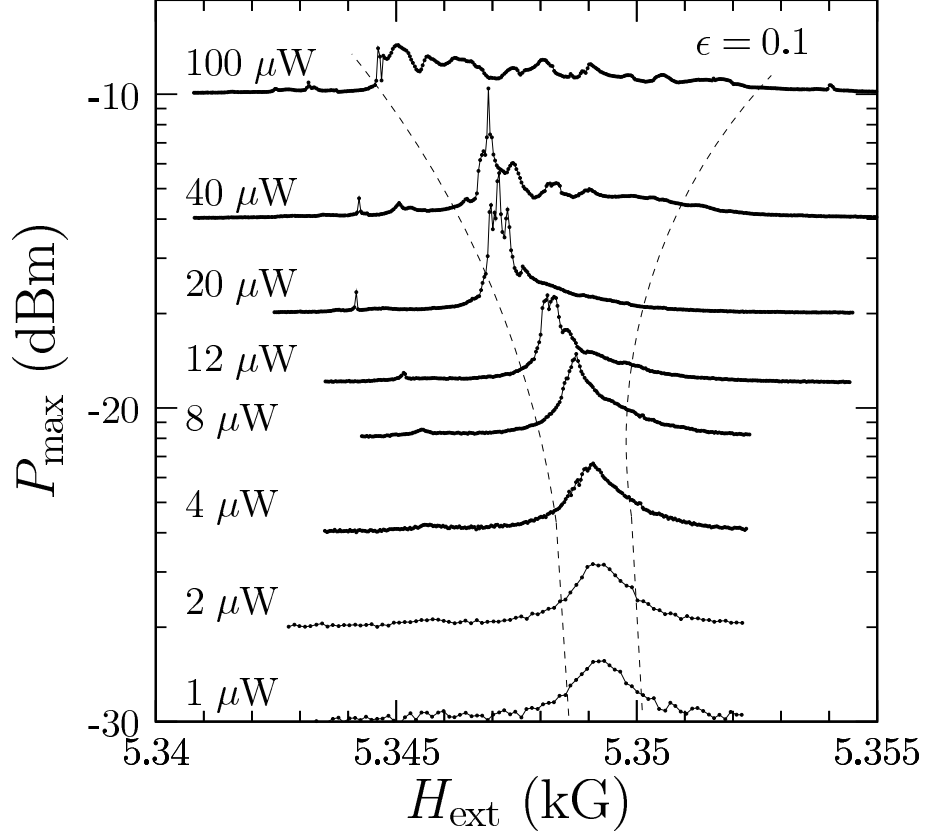


FIG. 3: Differential spectrum as a function of P_{\max} (constant $\epsilon = 0.1$).

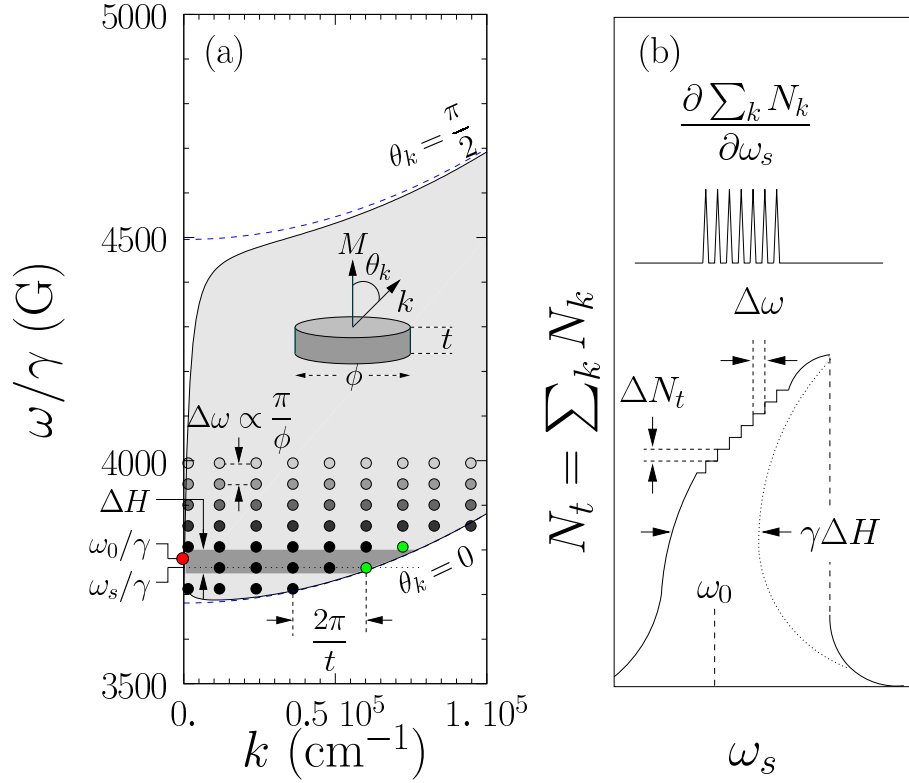


FIG. 4: (a) Magnon manifold of our perpendicularly magnetized YIG disk with a schematic of the mode discretisation induced by the confinement in a micron-size sample. Four-waves process couples the uniform mode (red) to the parametric modes at $\theta_k = 0$ (green) (b) Schematic of the distortion induced by the 4-waves NL process on the static spectroscopy of $M_z = \gamma\hbar \sum_k N_k$ vs. ω_s . The staircase behavior reveals the parametric spectrum in the differential characteristics.